JOURNAL OF AGRICULTURAL AND FOOD CHEMISTRY

Article

pubs.acs.org/JAFC

Control of Lipid Oxidation by Nonmigratory Active Packaging Films Prepared by Photoinitiated Graft Polymerization

Fang Tian, Eric A. Decker, and Julie M. Goddard*

Department of Food Science, University of Massachusetts, Chenoweth Lab, 102 Holdsworth Way, Amherst, Massachusetts 01003, United States

ABSTRACT: Transition metal-promoted oxidation impacts the quality, shelf life, and nutrition of many packaged foods. Metal-chelating active packaging therefore offers a means to protect foods against oxidation. Herein, we report the development and characterization of nonmigratory metal-chelating active packaging. To prepare the films, carboxylic acids were grafted onto the surfaces of polypropylene films by photoinitiated graft polymerization of acrylic acid. Attenuated total reflectance/Fourier transform infrared spectroscopy, contact angle, scanning electron microscopy, and iron-chelating assay were used to characterize film properties. Graft polymerization yielded a carboxylic acid density of 68.67 ± 9.99 nmol per cm^2 film, with ferrous iron-chelating activity of 71.07 ± 12.95 nmol per cm^2. The functionalized films extended the lag phase of lipid oxidation in a soybean oil-in-water emulsion system from 2 to 9 days. The application of such nonmigratory active packaging films represents a promising approach to reduce additive use while maintaining food quality.

KEYWORDS: *polypropylene, acrylic acid, photoinitiated graft polymerization, metal chelating, lipid oxidation inhibiting activity, active packaging film*

INTRODUCTION

Trace transition metals, especially iron, are strong prooxidants and have been reported to be involved in the initiation of lipid oxidation and the decomposition reaction of lipid primary oxidation products (lipid hydroperoxides).[1−5] In addition to promoting lipid oxidation, such metals are capable of initiating the oxidation of labile molecules such as antioxidants, carotenoids, and even essential amino acids by several different pathways. In fatty acid oxidation, transition metals, especially in their reduced state, promote the decomposition of hydroperoxides into reactive free radicals.[6] Hydroperoxides are ubiquitous to food lipids as a result of lipid oxidation promoted by oil extraction and refining and the incorporation of hydrogen peroxide as a preservative in some food products. The free radicals produced by hydroperoxide decomposition can then attack other labile molecules such as other fatty acids, antioxidants, and carotenoids, leading to their oxidative degradation. The ubiquitous existence of iron in foods, food ingredients, and water means that iron-promoted oxidation is a common problem in many food products. Chelators such as EDTA (ethylenediamine tetraacetic acid) and citric acid can bind free iron and decrease its ability to promote oxidative reactions. EDTA is the most effective food chelator used to maintain the quality and shelf life of salad dressings and mayonnaise due to the importance of the prooxidant activity of iron. A major drawback of utilizing EDTA in product formulations is the growing consumer demand for "all natural" label claims.[7,8] Most food companies therefore want to remove synthetic food additives from their products, and many attempts have been made to find natural replacements.

Antioxidant active packaging offers a novel approach to preserving food quality, in which the packaging material prevents oxidative degradation through the incorporation of active agents into or on the surface of the package.[9−12] Both synthetic and natural free radical scavengers can be blended into the packaging material,[13,14] but the resulting packaging is often costly and suffers from poor stability in terms of manufacturing and storing packaging materials. Furthermore, by incorporating the free radical scavengers throughout the packaging material, its bulk material properties (i.e., mechanical strength and optical clarity) can be adversely impacted. Likewise, synthetic free radical scavengers such as BHT (butylated hydroxytoluene) and BHA (butylated hydroxyanisole) are effective in inhibiting oxidation when coextruded in a packaging film[15,16] but are able to migrate from the package into the food product. The metal chelator EDTA also has been noncovalently incorporated into packaging substrates to prepare antioxidant packaging.[17,18] Such active packaging technologies that rely on migration of the synthetic active agents suffer regulatory challenges[19] and pose a potential concern to consumers seeking an "all natural" ingredient list.[7,8] The development of nonmigratory active packaging, in which the active agent is covalently linked to the packaging material, would therefore offer potential advantages in terms of both regulatory approval[19] and consumer acceptance. Herein, we report the development and characterization of a nonmigratory active packaging film, in which the metal chelator poly(acrylic acid) (PAA) is covalently grafted from the surface of polypropylene (PP) by photoinitiated graft polymerization.

There are two primary approaches to covalently graft polymer onto a planar substrate: grafting to and grafting from.[20] In the grafting-to technique, the inert substrate must undergo initial functionalization by creating active groups on

Received: March 6, 2012
Revised: July 11, 2012
Accepted: July 13, 2012
Published: July 13, 2012

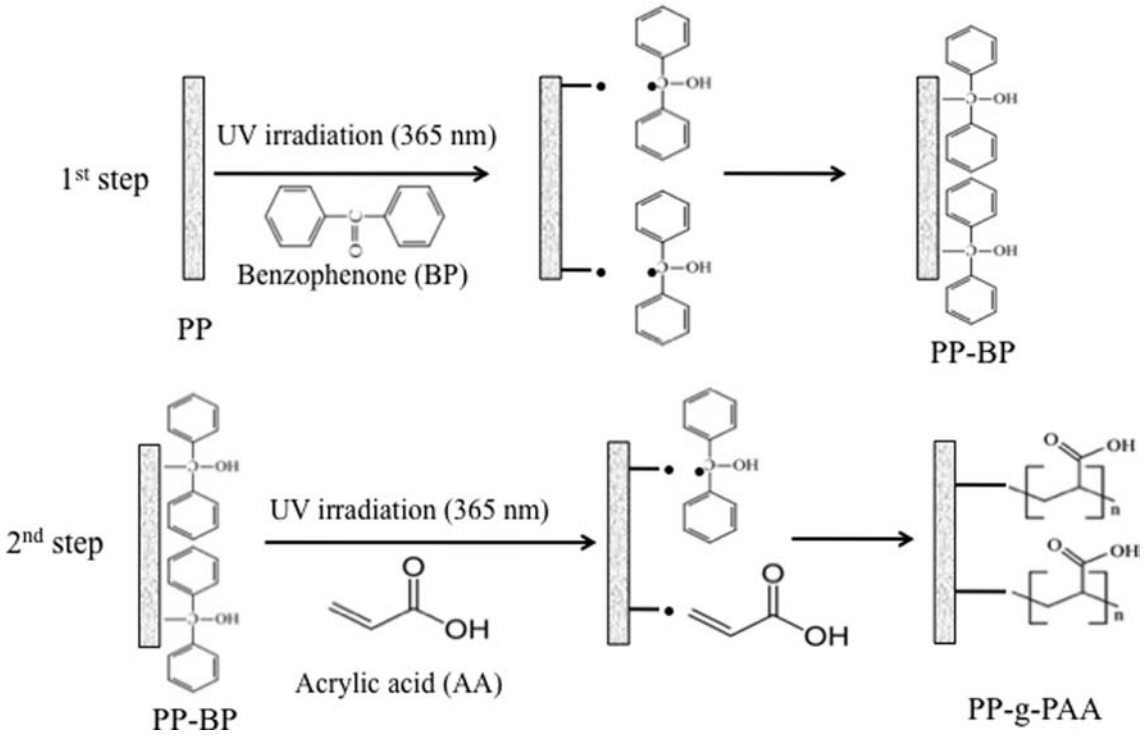

Figure 1. Sequential two-step reaction for the photoinitiated graft polymerization of AA onto the PP surface. The reaction route is adapted from ref 31.

the surface, after which the functional polymer is immobilized onto the surface, typically by wet chemical means. This technique has been successfully used to graft polymers onto substrates in the development of surface-modified materials in active packaging and other applications.[21−23] However, only a low-density brush (with correspondingly limited activity) can be yielded on the surface, which is a limitation of this method.[20] The grafting-from approach, also known as surface-initiated polymerization, is an alternative method in which high-density functional polymer brushes are grown from active sites on the substrate surfaces.[24] In recent years, photoinitiated graft polymerization has been exploited in a range of applications because it can be achieved quickly, at low cost, and active sites are generated simply by exposure to ultraviolet (UV) light.[20,24,25] Researchers have specifically investigated the grafting of acrylic acid monomer (AA) onto PP substrates, particularly membranes, by photoinitiated graft polymerization to improve their antifouling characteristics[26,27] or to prepare reversible adsorbents.[28,29] Another study photografted AA onto PP films for the binding of antifungal agents.[30] However, no research has been done to investigate the use of PAA grafted PP films (PP-g-PAA) in chelating transition metals with the goal of inhibiting metal-promoted oxidative degradation reactions such as lipid oxidation.

The goal of this research was to develop a nonmigratory metal-chelating PP film to control lipid oxidation. Functional AA monomer was grafted onto the PP film surface (grafted films are denoted as PP-g-PAA) by photoinitiated graft polymerization using UV irradiation to generate active sites for grafting. Attenuated total reflectance/Fourier transform infrared spectroscopy (ATR-FTIR), contact angle, scanning electron microscopy (SEM), atomic force microscopy (AFM), dye assay, and iron-chelating assay were used to characterize the surface properties of the films before and after AA grafting. Finally, the ability of the PP-g-PAA films to inhibit lipid oxidation was demonstrated using a soybean oil-in-water emulsion system.

MATERIALS AND METHODS

Materials. Commercial soybean oil (Wesson, 100% natural vegetable oil) was purchased from the local grocery store; PP (isotactic, pellets) was purchased from Scientific Polymer Products (Ontario, NY); hydroxylamine hydrochloride, ferrous sulfate heptahydrate (99+%), imidazole (99%), EDTA, and 3-(2-pyridyl)-5,6-diphenyl-1,2,4-triazine-*p*,*p*′-disulfonic acid disodium salt hydrate (ferrozine, 98+%) were purchased from Acros Organics (Morris Plains, NJ); toluidine blue O (TBO) was purchased from MP Biomedicals (Solon, OH); isopropyl alcohol, acetone, heptane, ethanol, isooctane, methanol, 1-butanol, sodium acetate trihydrate, 4-(2-hydroxyethyl)-1-piperazineethane-sulfonic acid (HEPES), hydrochloric acid, trichloroacetic acid (TCA), acetic acid glacial, Tween 20 (a nonionic surfactant), and sodium hydroxide were purchased from Fisher Scientific (Fair Lawn, NJ); AA (anhydrous), barium chloride dihydrate, ammonium thiocyanate, cumene hydroperoxide (80%), and benzophenone (BP, 99%) were purchased from Sigma-Aldrich (St. Louis, MO); all of the chemicals and solvents were used without further purification.

Preparation of PP Films. PP films with an average thickness of 225 ± 25 μm were prepared with a Carver Laboratory Press (model B, Fred S. Carver Inc., NJ). PP pellets were cleaned by sonicating in isopropyl alcohol, acetone, and deionized water (10 min per repetition, 2 repetitions per solvent) sequentially. The cleaned PP pellets were dried overnight over anhydrous calcium sulfate at room temperature (25 °C). The temperature of the Carver Press was set to 160 °C to melt PP pellets for 1 min, and 9000 lb of pressure was then loaded to press pellets into films. Pressed films were cut to 1 × 2 cm^2 pieces, cleaned, and dried by the same procedure as the PP pellets. Typical commercial films contain a number of additives, including antioxidants, which may interfere with the graft polymerization process and subsequent antioxidant activity assays. Because the specific nature of these additives is unknown in commercial films,

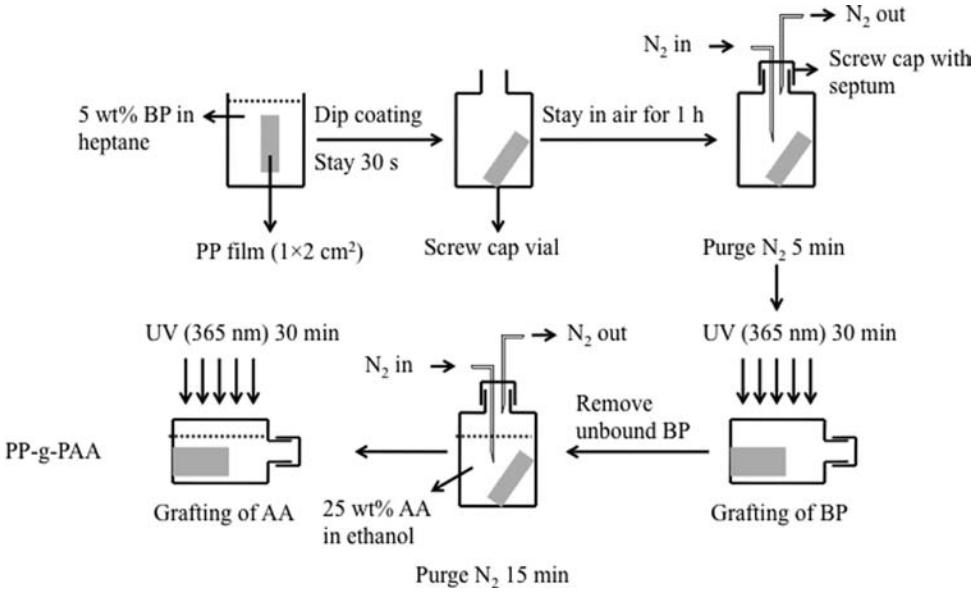

Figure 2. Procedure scheme for the two-step photoinitiated graft polymerization of AA from the PP surface.

films in this study were prepared from polymer resins purchased from a polymer supply company (Scientific Polymer Products, Ontario, NY) to minimize the effect of such additives on the surface modification and antioxidant activity assays. Resins and heat-pressed films were extensively cleaned to remove organic contaminants that commonly deposit from the environment (even during careful, clean handling), which may interfere with accurate surface analysis. It should be noted that the films prepared in this study were thicker than typical food-packaging films. Indeed, the thickness of the films is simply for ease of handling films during experimentation—because the modifications are limited to the surface and the antioxidant activity occurs at the interface of the film and the emulsion, the thickness should not impact the results of the study.

Preparation of PP-g-PAA Films by Photoinitiated Graft Polymerization. A two-step sequential photoinitiated graft polymerization was used to graft AA onto the PP surface using an adaptation of the methods reported by Ma et al.[31] and Janorkar et al.[32] In the first step, the photoinitiator BP was covalently grafted to the PP surface, and the graft polymerization of AA from the PP surface was initiated in the second step (Figure 1). A schematic of the two-step graft polymerization procedure is depicted in Figure 2. While it is also possible to perform a one-step photoinitiated graft polymerization, foregoing the BP step, the BP surface initiation step ensures that the grafted PAA is covalently bound to the PP film and not just a cross-linked PAA coating. This is an important distinction for the application of active food packaging, for which covalent immobilization may be an important regulatory advantage.

In the first step, PP films were dip-coated in a 5 wt % solution of BP in heptane for 30 s to coat the outermost surface of the films with the photoinitiator. The BP-coated film was then put into a headspace vial and left open for 1 h to allow for the evaporation of residual heptane. The vial was then closed with a screw cap fitted with a septum. Nitrogen was then purged into the sealed vial for 5 min to eliminate any oxygen that would inhibit the photoactivation of the BP and the subsequent grafting. The nitrogen purged vial was then transferred into a nitrogen glovebag equipped with a 100 W Black-Ray UV lamp with spot bulb (TED PELLA, Inc., CA). A black light filter is recessed in the head of the UV lamp, which delivers long-wave (365 nm) UV light with an intensity of 21.7 mW/cm^2 at a distance of 5 cm. The BP-coated films were irradiated in the nitrogen-purged vials for 30 min to covalently graft BP to the surface of PP films. After irradiation, the films were removed from the vials and washed three times in acetone (5 min per time). The BP-activated PP films (PP-BP) were then dried in air at room temperature.

In the second step of the graft polymerization procedure, the PP-BP films were submerged in a solution of AA monomer in ethanol (25 wt % AA) and again sealed in septum-capped vials. Nitrogen was purged into the monomer solution for 15 min to eliminate any oxygen. Vials were then put into the nitrogen glovebag and exposed to UV irradiation for 30 min. The AA-grafted films (PP-g-PAA) were washed in deionized water with stirring using the method reported by Ulbricht et al.[28] to completely remove the unreacted AA monomer and homopolymer generated in the photoinitiated polymerization process. Briefly, films were submerged in deionized water with stirring for 30 min at room temperature, then stirred in a second beaker of fresh deionized water for 1 h at 60 °C, and finally stirred in a third beaker of fresh deionized water for 30 min at room temperature. The grafted, washed PP-g-PAA films were then dried overnight at room temperature over anhydrous calcium sulfate before further use or analysis.

ATR-FTIR Analysis. ATR-FTIR analysis of the modified and unmodified PP film surfaces was carried out on an IRPrestige-21 FTIR spectrometer (Shimadzu Scientific Instruments, Inc., Kyoto, Japan) with sample compartments and a diamond ATR crystal. At a 4 cm^{-1} resolution, 32 scans were done for each spectrum against a reference spectrum of an empty ATR crystal. The resultant spectra were processed with SigmaPlot 10.0 (Systat Software, Inc., Chicago, IL) and analyzed with KnowItAll Informatics System 8.1 (BioRad, Hercules, CA).

Contact Angle Analysis. The surface hydrophilicity of PP, PP-BP, and PP-g-PAA films was determined by measuring water contact angles on a DSA 100 (Kruss, Hamburg, Germany) equipped with a direct dosing system (DO3210, Kruss, Hamburg, Germany). All measurements were conducted under atmospheric conditions with high-performance liquid chromatography grade deionized water (Fisher Scientific, Fair Lawn, NJ) as the probe liquid. Angles were recorded every 0.10 s during measurements and calculated using tangent method 2. The reported advancing and receding contact angles represent the averages of six measurements, which were taken on three independent films.

SEM Analysis. The surface and cross-sectional morphologies of PP and PP-g-PAA films were obtained by field emission SEM (JEOL 6320 FXV). The films for SEM analysis were freeze-fractured in liquid nitrogen to observe their cross-sectional morphology. Samples were sputter-coated (Sputter coater, Cressington 108) with gold for 3 min before SEM analysis.

AFM Analysis. The surface topography of PP and PP-g-PAA films was analyzed by AFM (Digital Instruments, Dimension-3000 model) with a NanoScope IIIa controller. Tapping mode images of films in air

were obtained using a silicon cantilever tip (uncoated, AppNano ACT-R-W type) with a spring constant of 40 N/m. The scan size was 50 μm × 50 μm for each sample, and roughness was calculated as the root-mean-square (rms) roughness.

Quantification of Carboxylic Acids. The amount of available carboxylic acids on PP and PP-g-PAA surface was measured by the TBO dye assay reported by Kang et al.[33] and Uchida et al.[34] with some modifications. PP and PP-g-PAA films were submerged in 5 mL of 0.5 mM TBO solution (in deionized water solution adjusted to pH 10.0 by NaOH) at 25 °C for 2 h. Noncomplexed dye was removed by rinsing films in NaOH solution (pH 10.0) three times. The films were then submerged in 50 wt % acetic acid solution for 15 min to desorb the complexed dye on film surfaces. The absorbance of the acetic acid solution containing desorbed dye was detected at 633 nm. The carboxylic acid density of the film surface was calculated by comparison to a standard curve made of TBO dye in 50 wt % acetic acid solution.

Iron-Chelating Assay. The ability of PP and PP-g-PAA films to chelate Fe^{2+} iron was determined using the colorimetric ferrozine assay reported by Bou et al.[35] with some modifications. Ferrous iron solution (1 mM) was prepared by adding ferrous sulfate heptahydrate solution (20 mM, in 0.05 M HCl) into a sodium acetate/imidazole buffer (0.05 M, pH 5.0). PP or PP-g-PAA films were submerged into the iron solution for 30 min to chelate iron and then washed thoroughly in deionized water. Chelated iron was released by submerging films in releasing agent (0.1 g/mL of $HONH_2$·HCl and 0.05 g/mL of TCA) for 2.5 h. The releasing agent (0.5 mL) then reacted with ferrozine solution (0.5 mL, 9.0 mM, in 50 mM HEPES buffer, pH 7.0) for 1 h, and the absorbance was detected at 562 nm. The iron-chelating activity was determined by comparison to a standard curve made from ferrous sulfate heptahydrate.

Lipid Oxidation Assay. The effectiveness of the iron-chelating PP-g-PAA films in preventing lipid oxidation was determined using an oil-in-water emulsion system stored at 37 °C. Unmodified PP films and PP-g-PAA films were incubated with rotation in an oil-in-water emulsion, stabilized by Tween 20. Generation of lipid oxidation products (lipid hydroperoxides and hexanal) was quantified over time and compared to that of a sample of emulsion with no film (negative control) as well as an EDTA-containing emulsion as a positive control. Four independent preparations served as the replicates, and results are representative of oxidation data collected on two independent days.

A coarse emulsion consisting of 1 wt % soybean oil and an aqueous solution of 0.1 wt % Tween 20 and 50 mM sodium acetate/imidazole buffer (pH 7.0) was made by blending for 2 min using a two-speed BioHomogenizer (Biospec Products, Inc., Bartlesville, OK) at the low speed setting (7000 rpm). The coarse emulsion was then passed four times through a Microfluidics (Newton, MA) at 9000 psi. The particle size distribution of the emulsion droplets was determined by laser diffraction (Mastersizer 2000 Particle Size Analyzer, Malvern Instruments Ltd., Worcestershire, United Kingdom). The final average droplet diameter of the emulsion (D_{32}) was determined to be 0.159 ± 0.004 μm, which did not change during the storage study. The EDTA-containing emulsion was prepared by dissolving EDTA in sodium acetate/imidazole buffer (50 mM, pH 7.0) followed by addition to the emulsion to a final concentration of 0.01 mM EDTA. Emulsions (1 mL) were added into screw-capped glass vials and incubated in the dark incubator with shaking at 37 °C for 14 days. Four pieces (1 × 1 cm^2) of unmodified PP or modified PP-g-PAA films were placed into vials containing 1 mL of emulsion to measure their ability to inhibit lipid oxidation.

Lipid hydroperoxides, the primary lipid oxidation products, were quantified using an adaptation of the colorimetric ammonium thiocyanate method from Shantha et al.[36] and Alamed et al.[37] Emulsion (0.3 mL) was added to 1.5 mL of isooctane/isopropanol (3:1 v/v) and vortexed three times (10s per time). The mixed solution was separated by a centrifuge (model 225A, Fisher Scientific, Dubuque, IA) at the maximum speed (3400g) for 5 min. The upper phase (200 μL) was then mixed with 2.8 mL of methanol/1-butanol (2:1 v/v), 15 μL of ammonium thiocyanate (3.94 M), and 15 μL of ferrous iron solution. The clear ferrous iron solution was prepared by centrifugation (1000 rpm, 2 min) of a mixture of equal amount of 0.132 M $BaCl_2$ (in 0.4 M HCl) and 0.144 M $FeSO_4$. The absorbance of the reaction solution was detected at 510 nm after 20 min of incubation at room temperature. Hydroperoxide concentrations were calculated by comparison to a standard curve made from cumene hydroperoxide. The lag phase of the lipid hydroperoxide formation in emulsions was defined as the day before which the hydroperoxide concentration significantly increased as compared to initial concentrations ($P < 0.05$).

The amount of hexanal in the headspace of the vial was determined according to the method described by Panya et al.[38] using a gas chromatograph (GC, Shimadzu GC-2014, Tokyo, Japan) equipped with an autoinjector (AOC-5000, Shimadzu, Tokyo, Japan) and a flame ionization detector (FID). The sample vial was warmed up at 55 °C for 8 min. A divinylbenzene/carboxen/polydimethylsiloxane (DVB/Carboxen/PDMS) stable flex SPME fiber (50/30 μm, Supelco, Bellefonte, PA) was then inserted into the vial and exposed to the sample headspace for 2 min. The fiber was desorbed in the detector for 3 min at a split ratio of 1:7. The chromatographic separation of volatile lipid oxidation compounds was performed on a fused-silica capillary column (30 m × 0.32 mm i.d. × 1 μm) coated with 100% poly(dimethylsiloxane) (Equity-1, Supelco). The temperatures of the oven, injector, and detector were 65, 250, and 250 °C, respectively. The run time for each sample was 10 min. The concentration of hexanal was calculated according to the standard curve made from emulsions containing known amounts of hexanal and 0.2 mM EDTA. The lag phase of the hexanal formation in emulsions was defined as the day before which the hexanal concentration significantly increased as compared to initial concentrations ($P < 0.05$).

Statistical Analysis. The data presented are means ± standard deviations (SDs) of at least four replicate determinations, from four preparations of film. To prepare samples for each determination, individual films (1 × 2 cm^2) were placed in separate, independent vials to perform the grafting of initiator/monomer. Reported results are representative of results of two independent studies performed on different days. SPSS Release 17.0 (SPSS Inc., Chicago, IL) was used to perform statistical analyses. One-way analysis of variance (ANOVA) followed by Duncan's pairwise comparison was conducted to determine differences ($P < 0.05$).

RESULTS AND DISCUSSION

Photoinitiated Graft Polymerization and Surface Characterization of PP-g-PAA. A two-step sequential photoinitiated graft polymerization of AA from the surface of PP films was used to introduce metal-chelating carboxylic acids as an active packaging technology (Figure 1). In the first step, the photoinitiator BP undergoes photoinduced excitation after exposure to UV irradiation, and the excited BP can then abstract the tertiary hydrogen from the PP film surface to generate surface radicals and semipinacol radicals. In the absence of monomers, these two radicals then react to form BP surface initiators.[31] In the second step, the C−C bond of the BP surface initiator formed in the first step is cleaved by UV irradiation to regenerate surface radicals and semipinacol radicals.[27] The surface radicals are then available to attack the C═C of the AA monomer to initiate the graft polymerization. It has been reported that the semipinacol radicals prefer to combine with growing polymeric chain radicals. After termination, the semipinacol can split off to reinitiate the polymerization and then to increase the polymer chain length.[31]

ATR-FTIR spectroscopy was performed on control and modified films to evaluate the surface chemistry at various points in the graft polymerization process (Figure 3). A new absorption band at 690−710 cm^{-1} (Figure 3B), characteristic absorbance corresponding to the aromatic ring from BP, was observed in the spectra of PP-BP. This indicated that BP was successfully grafted to the PP surface in the first step. Two new

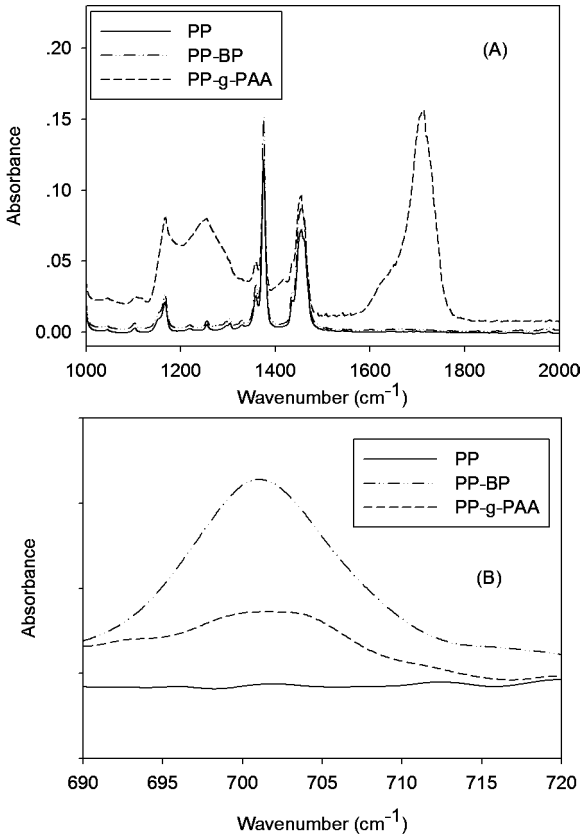

Figure 3. ATR-FTIR spectra of PP, PP-BP, and PP-g-PAA films in the range of (A) 1000−2000 and (B) 690−720 cm^{-1}. Spectra shown here are representative of four replications collected from two independent films per treatment.

strong absorbance bands were observed in the spectra of PP-g-PAA (Figure 3A). One is at 1700−1725 cm^{-1}, which is attributable to the C═O of carboxylic acids. The other one is the C−O band of carboxylic acids at 1211−1320 cm^{-1}. These indicated the successful grafting of the PAA chain onto the PP surface. In Figure 3B, a significant decrease of the absorbance at 690−710 cm^{-1} was evident in the spectra of PP-g-PAA as compared to PP-BP. This confirmed the cleavage of the C−C bond of the surface initiator, confirming successful initiation of graft polymerization by the surface radicals in agreement with the report of Ma et al.[31]

The advancing and receding water contact angles of the native and modified PP films were measured to determine the effect of AA grafting on the hydrophilicity of film surfaces (Table 1). Both the advancing and the receding angles of native PP films were very high, with low hysteresis, indicating a clean, hydrophobic surface. After the grafting of BP, the advancing angle of the film surface had no difference with that of the native PP film surface, while the receding angle was lower. This increase in hysteresis indicates successful introduction of the reactive BP active sites, which introduce slight polarity to the surface. The advancing and receding angles decreased after the grafting of PAA, especially the receding angle, which decreased by more than 60 degrees as compared to the PP and PP-BP films. These results indicate a significant increase in surface hydrophilicity of PP-g-PAA, likely a result of the introduction of polar, ionizable carboxylic acids as confirmed by FTIR spectra and dye assay analysis, discussed below. As expected, the hysteresis of PP-g-PAA was much higher than that of PP and PP-BP. The increase in surface roughness, surface chemical heterogeneity, and the increased interactions between the surface and the water droplet after the grafting of flexible PAA graft chains likely influenced this high hysteresis.[39,40]

Table 1. Water Contact Angle of PP, PP-BP, and PP-g-PAA Films[a]

contact angle	advancing (deg)	receding (deg)	hysteresis (deg)
PP	105.9 ± 1.2 a	87.7 ± 2.3 a	18.2
PP-BP	106.6 ± 1.8 a	81.6 ± 1.3 b	25.0
PP-g-PAA	74.8 ± 4.7 b	18.3 ± 5.0 c	56.5

[a]Values are averages ± standard deviations ($n = 6$). Different letters in the same column indicate significant differences ($P < 0.05$).

Surface and cross-sectional SEM images as well as AFM images were obtained to evaluate morphology of control and modified films (Figures 4 and 5). Both the surface and the cross-sectional SEMs of native PP film suggested a uniform morphology with no noticeable defects (Figure 4A,C). The surface of PP-g-PAA presented a cracklike morphology (Figures 4B and 5B). This cracklike surface morphology is in agreement with other reports, which suggest that the grafted hydrophilic polymers shrink and crack upon drying. Fasce et al.[41] reported a similar morphology of PP and PAA grafted PP surfaces by SEM. Aside from the evident cracking, the surface morphology was uniform, indicating uniform grafting across the surface. The uniformity of the grafted PAA was determined by taking SEMs at three points on cross-sections of three independently prepared PP-g-PAA films and measuring the thickness of the graft and was determined to be 17.6 ± 4.4 μm. A representative cross-sectional SEM is depicted in Figure 4D. The cross-sectional SEM of PP-g-PAA films exhibits two distinct phases, in which the left-most surface layer (PAA graft) shows a different texture with the substrate material. The absence of a clear, sharp interface between PP substrate and PAA graft indicates that some BP initiator and subsequent AA monomer penetrated the surface of the PP film, further supporting that delamination of the active PAA graft from the PP substrate is unlikely.

Surface roughness of PP and PP-g-PAA films was quantified using AFM on dried samples (Figure 5). The surface of unmodified PP film (Figure 5A) exhibited some degree of roughness (calculated rms roughness value of 57.856 nm), which is likely due to scratches obtained during hot pressing and washing. In agreement with the SEM images, AFM images revealed a cracklike surface morphology on the PP-g-PAA film surface (Figure 5B). This suggests that these cracks are likely a result of the shrinking of highly hydrophilic PAA polymers under dry condition. After grafting, the surface roughness of PP-g-PAA was more than two times higher than that of PP control, which further explains the high contact angle hysteresis.

Dye Assay. TBO dye assay was performed to quantify the carboxylic acid density on the surface of PP and PP-g-PAA films. The dye assay not only can quantify the amount of the available carboxylic acids grafted onto the PP surface, but it also provides a qualitative indication of the surface uniformity of the grafting by color. Hence, it can provide more information about the surface grafting than the gravimetric method commonly used in prior research.[27,41,42] A layer of blue color dye was observed uniformly distributed on the PP-g-PAA film surface after the adsorption reaction in basic TBO dye solution,

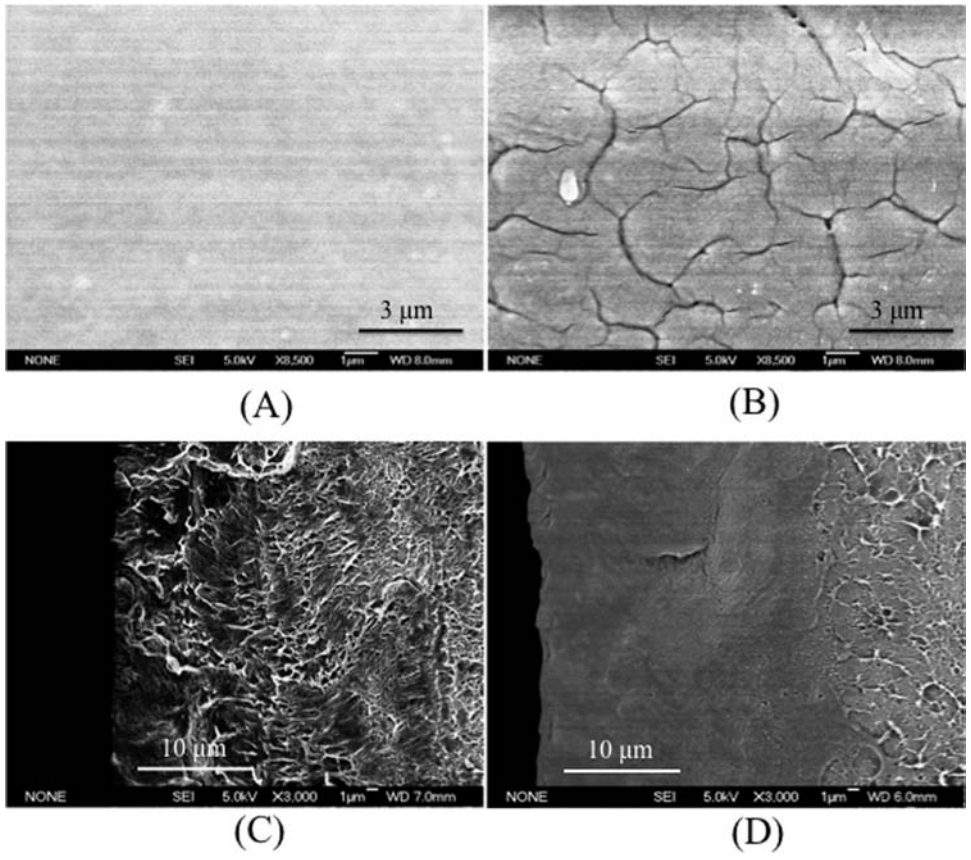

Figure 4. SEM images of the (A) PP film surface, (B) PP-g-PAA film surface, (C) PP film cross-section, and (D) PP-g-PAA film cross-section.

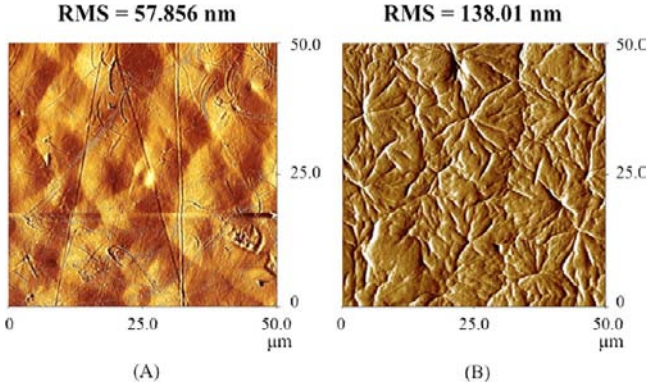

Figure 5. AFM amplitude images and rms roughness of the (A) PP film surface and (B) PP-g-PAA film surface.

indicating a uniform grafting of PAA on PP film surface. Following photoinitiated grafting of AA, a large amount of available carboxylic acids was detected on the surface of PP-g-PAA film (68.67 ± 9.99 nmol/cm^2), which dramatically increased as compared to the native PP film (0.12 ± 0.01 nmol/cm^2). This confirmed the successful grafting of AA on the PP film surface and is substantially higher in carboxylic acid density as compared to prior reports, which use a wet chemical grafting-to method.[21,43]

Ferrous Iron-Chelating Activity. The ability of PP and PP-g-PAA films to chelate ferrous ions was determined using a modified ferrozine assay. The PP-g-PAA film exhibited significantly greater ferrous iron-chelating activity (71.07 ± 12.95 nmol/cm^2) as compared to the PP film (0.31 ± 0.30 nmol/cm^2). As the carboxylic acid density of the PP-g-PAA film is 68.67 ± 9.99 nmol/cm^2, the ligand (carboxylic acid) to metal (Fe^{2+}) ratio is approximately 1. The theoretical ligand to metal binding ratio for carboxylic acids and ferrous ions is 2, in which two carboxylic acids bind four of the six coordination sites of iron and balance the two positive charges.[21,43] In this structure, two water molecules bind the remaining two coordination sites to form the most stable octahedral complex structure (Figure 6A).[44,45] When bound in this manner, ferrous ions are completely enveloped and lose their ability to catalyze oxidative degradation reactions like lipid oxidation. There are two potential explanations for achieving a ligand/metal ratio near 1 as observed in this study. It has been reported that ligand–metal complexes with a net cationic charge can be formed in a 1:1 ratio of COOH:Fe^{2+} as illustrated in Figure 6B.[46,47] It is also possible that the steric restriction of the PP substrate and the surrounding carboxylic acids in the PAA grafts inhibit the formation of an octahedral complex structure.[48] Therefore, it is possible to "incompletely" bind iron ions by less than the six total coordination sites. In this case, while the metal ions retain some activity, it will be inhibited to some extent. Moreover, as an active packaging film, even incomplete binding of iron ions will result in their physical separation from the food matrix, which offers an additional means to inhibit lipid oxidation.

Lipid Oxidation Inhibiting Activity. Lipids are susceptible to oxidative degradation, a major cause of food quality deterioration. Lipid hydroperoxides are the main products in the early stages of oxidation. These primary oxidation products are unstable and prone to decomposition to secondary oxidation products, which are a complex mixture of volatile, nonvolatile, and polymeric compounds. Hexanal is an

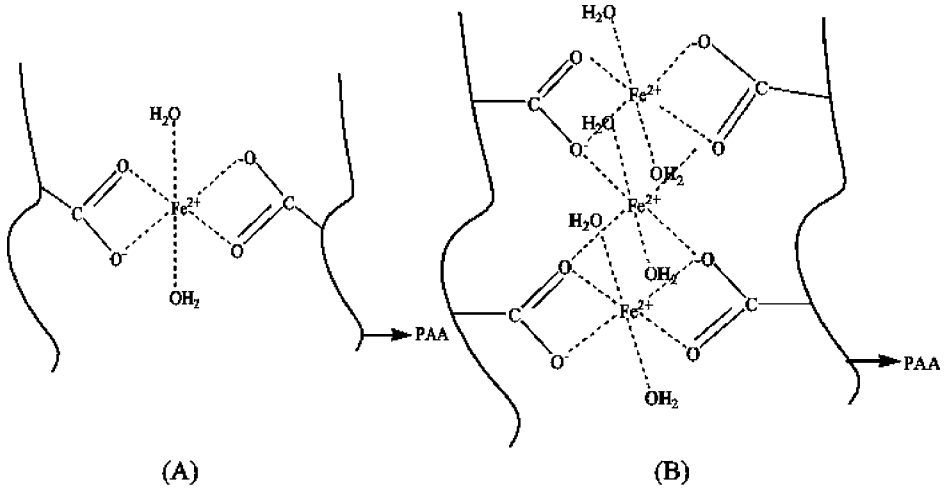

Figure 6. Octahedral structure of the carboxylic acid/Fe^{2+} complex with the ligand/metal ratio being 2 (A) and 1 (B).

important volatile aldehyde decomposed from hydroperoxides of ω-6 fatty acids, the predominant unsaturated fatty acids in soybean oil. In this study, the formation of hydroperoxides and hexanal of oil-in-water emulsions alone, with unmodified PP film, with PP-g-PAA film, and with added EDTA as a positive control, was measured during storage at pH 7.0 to quantify the ability of the PP-g-PAA active packaging films to inhibit lipid oxidation (Figure 7).

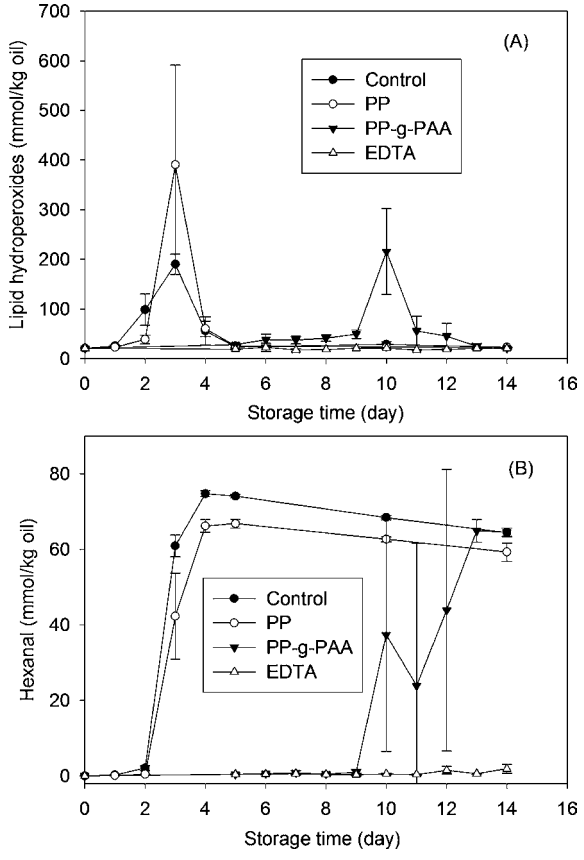

Figure 7. Lipid hydroperoixdes (A) and hexanal (B) concentrations of soybean oil-in-water emulsion stored at 37 °C and measured over 14 days.

Lipid oxidation occurred rapidly in the oil-in-water emulsion control, with a lag phase of lipid hydroperoxides and hexanal formation of 1 and 2 days, respectively. The emulsion incubated with PP also oxidized quickly, with a lag phase of both lipid hydroperoxides and hexanal formation of 2 days. As expected, the EDTA positive control effectively inhibited lipid oxidation for the duration of the study. Lipid oxidation was also strongly inhibited by the PP-g-PAA films, in which the lag phase of lipid hydroperoxides and hexanal formation was extended to 9 days. The results of the lipid oxidation experiments, in conjunction with those of the dye assay and iron-chelating assays, indicate that PP-g-PAA films are effective in inhibiting the oxidation of oil-in-water emulsions by chelation of prooxidant ferrous ions.[38]

Conclusions. A nonmigratory metal-chelating active packaging film with antioxidant activity was successfully prepared by the photoinitiated graft polymerization of AA onto PP film surface. The grafted PAA layer significantly increased the hydrophilicity of PP films and had a thickness of 17.6 ± 4.4 μm. The polymerization reaction yielded grafted carboxylic acids of 68.67 ± 9.99 nmol per cm^2 film surface, with ferrous iron-chelating activity of 71.07 ± 12.95 nmol per cm^2 film surface. As compared to the native PP films, PP-g-PAA films effectively inhibited lipid oxidation in a soybean oil-in-water emulsion system, dramatically extending the lag phases of the formation of lipid hydroperoxides and hexanal from 2 to 9 days.

Preliminary calculations were performed to estimate how the reported film-chelating capacity compares to an equivalent concentration of EDTA in a model-packaged product system. The total surface area of a typical half gallon (1.89 L) carton is approximately 960 cm^2. A model package of those dimensions made with our film (iron-chelating capacity of 71.07 nmol/cm^2) can therefore chelate 68.2 μmol iron. As 2 mol of EDTA is needed to bind 1 mol of iron, this correlates to 136.5 μmol EDTA or 72.2 μM EDTA for the model 1.89 L carton. It has been reported that the concentration of EDTA required to dramatically decrease lipid oxidation is only 2.5 μM.[37] The maximum concentration of EDTA permitted by the FDA to be added into beverages is 33 ppm, which is 113 μM.[49] The PP-g-PAA films reported in this paper have an equivalent chelating activity of 72.2 μM EDTA, which is well above the minimum concentration of EDTA required to inhibit lipid oxidation (2.5 μM) and on the order of, but below, the FDA maximum (113 μM).

It is important to note that while the materials developed herein have been shown to be effective in inhibiting lipid oxidation by chelating trace iron, these materials would not be suitable for foods that are an important nutritional source of iron. Ongoing research is evaluating the influence of complex food matrices on the performance of the iron-chelating active packaging materials and to better identify food systems for which the PP-g-PAA films perform best in inhibiting lipid oxidation. Furthermore, a rigorous evaluation of migration into foodstuff and food simulants must be performed to confirm the nonmigratory nature of the developed active packaging materials. Adaptation of the benchtop process to roll-to-roll processing schemes is the subject of ongoing research in our laboratories and is also critical to the translational success of our lab-scale process into commercial application.

The PP-g-PAA films developed and characterized in this publication offer a novel means to inhibit transition metal-promoted oxidation of important nutritional and quality factors in packaged foods. The covalent surface-initiated graft polymerization technique is a novel means to generate nonmigratory active packaging films at a low cost. Development of such an effective and economical active packaging film represents a promising means by which to reduce additive use in food industry while maintaining high food quality.

AUTHOR INFORMATION

Corresponding Author

*Tel: 413-545-2275. Fax: 413-545-1262. E-mail: goddard@foodsci.umass.edu.

Funding

Portions of this work were supported by the Center for Hierarchical Manufacturing, an NSF Nanoscale Science & Engineering Center supported by the National Science Foundation under NSF Grant No. CMMI-0531171, and in part by the U.S. Department of Agriculture National Institute of Food and Agriculture.

Notes

The authors declare no competing financial interest.

ACKNOWLEDGMENTS

We gratefully acknowledge Jean Alamed and Panya Atikorn for experimental design support for the lipid oxidation experiments, Dr. D. Julian McClements for use of his Kruss DSA100 and emulsion preparation equipment, and Dr. Sekar Dhanasekaran for performing AFM analysis in the W. M. Keck Nanostructures Laboratory.

REFERENCES

(1) Mancuso, J.; McClements, D.; Decker, E. Iron-accelerated cumene hydroperoxide decomposition in hexadecane and trilaurin emulsions. *J. Agric. Food Chem.* **2000**, *48*, 213−219.

(2) Mei, L.; Decker, E.; McClements, D. Evidence of iron association with emulsion droplets and its impact on lipid oxidation. *J. Agric. Food Chem.* **1998**, *46*, 5072−5077.

(3) Yoshida, Y.; Niki, E. Oxidation of methyl linoleate in aqueous dispersions induced by copper and iron. *Arch. Biochem. Biophys.* **1992**, *295*, 107−114.

(4) Huang, S.; Frankel, E.; German, J. Antioxidant activity of alpha-tocopherols and gamma-tocopherols in bulk oils and in oil-in-water emulsions. *J. Agric. Food Chem.* **1994**, *42*, 2108−2114.

(5) Chaiyasit, W.; Elias, R. J.; McClements, D. J.; Decker, E. A. Role of physical structures in bulk oils on lipid oxidation. *Crit. Rev. Food Sci. Nutr.* **2007**, *47*, 299−317.

(6) Leopoldini, M. Iron chelation by the powerful antioxidant flavonoid quercetin. *J. Agric. Food Chem.* **2006**, *54*, 6343−6351.

(7) Levine, M. Natural and organic food and beverage trends in the U.S.—Current and future patterns in production, marketing, retailing, and consumer usage. *Packaged Facts* **2008**, 1−225.

(8) Dowd, T. Natural and organic personal care products in the U.S. *Packaged Facts* **2007**, 1−311.

(9) Brody, A.; Bugusu, B.; Han, J.; Sand, C.; Mchugh, T. Innovative food packaging solutions. *J. Food Sci.* **2008**, *73*, R107−R116.

(10) Nerin, C.; Tovar, L.; Salafranca, J. Behaviour of a new antioxidant active film versus oxidizable model compounds. *J. Food Eng.* **2008**, *84*, 313−320.

(11) Gemili, S.; Yemenicioglu, A.; Altinkaya, S. Development of antioxidant food packaging materials with controlled release properties. *J. Food Eng.* **2010**, *96*, 325−332.

(12) Pereira de Abreu, D. A.; Paseiro Losada, P.; Maroto, J.; Cruz, J. M. Evaluation of the effectiveness of a new active packaging film containing natural antioxidants (from barley husks) that retard lipid damage in frozen Atlantic salmon (*Salmo salar* L.). *Food Res. Int.* **2010**, *43*, 1277−1282.

(13) Bentayeb, K.; Rubio, C.; Batlle, R.; Nerin, C. Direct determination of carnosic acid in a new active packaging based on natural extract of rosemary. *Anal. Bioanal. Chem.* **2007**, *389*, 1989−1996.

(14) Camo, J.; Lores, A.; Djenane, D.; Antonio Beltran, J.; Roncales, P. Display life of beef packaged with an antioxidant active film as a function of the concentration of oregano extract. *Meat Sci.* **2011**, *88*, 174−178.

(15) Soto-Cantu, C. D.; Graciano-Verdugo, A. Z.; Peralta, E.; Islas-Rubio, A. R.; Gonzalez Cordova, A. Release of butylated hydroxytoluene from an active film packaging to Asadero cheese and its effect on oxidation and odor stability. *J. Dairy Sci.* **2008**, *91*, 11−19.

(16) Byun, Y.; Kim, Y.; Whiteside, S. Characterization of an antioxidant polylactic acid (PLA) film prepared with alpha-tocopherol, BHT and polyethylene glycol using film cast extruder. *J. Food Eng.* **2010**, *100*, 239−244.

(17) Gucbilmez, C. M.; Yemenicioglu, A.; Arslanoglu, A. Antimicrobial and antioxidant activity of edible zein films incorporated with lysozyme, albumin proteins and disodium EDTA. *Food Res. Int.* **2007**, *40*, 80−91.

(18) Unalan, I.; Korel, F.; Yemenicioglu, A. Active packaging of ground beef patties by edible zein films incorporated with partially purified lysozyme and Na(2)EDTA. *Int. J. Food Sci. Technol.* **2011**, *46*, 1289−1295.

(19) Anonymous. *Code of Federal Regulations*; U.S. Government Printing Office: Washington, DC, 2005; Title 21, Parts 170−199.

(20) Dyer, D. Photoinitiated synthesis of grafted polymers. *Adv. Polym. Sci.* **2006**, *197*, 47−65.

(21) Goddard, J. M.; Hotchkiss, J. H. Tailored functionalization of low-density polyethylene surfaces. *J. Appl. Polym. Sci.* **2008**, *108*, 2940−2949.

(22) Goddard, J. M.; Talbert, J. N.; Hotchkiss, J. H. Covalent attachment of lactase to low-density polyethylene films. *J. Food Sci.* **2007**, *72*, E36−E41.

(23) Barish, J.; Goddard, J. Polyethylene glycol grafted polyethylene: A versatile platform for nonmigratory active packaging applications. *J. Food Sci.* **2011**, *76*, E586−E591.

(24) Edmondson, S.; Osborne, V. L.; Huck, W. T. S. Polymer brushes via surface-initiated polymerizations. *Chem. Soc. Rev.* **2004**, *33*, 14−22.

(25) Yagci, Y.; Jockusch, S.; Turro, N. Photoinitiated polymerization: advances, challenges, and opportunities. *Macromolecules* **2010**, *43*, 6245−6260.

(26) Ulbricht, M. Photograft-polymer-modified microporous membranes with environment-sensitive permeabilities. *React. Funct. Polym.* **1996**, *31*, 165−177.

(27) Yu, H. Y.; Xu, Z. K.; Yang, Q.; Hu, M. X.; Wang, S. Y. Improvement of the antifouling characteristics for polypropylene

microporous membranes by the sequential photoinduced graft polymerization of acrylic acid. *J. Membr. Sci.* **2006**, *281*, 658−665.
(28) Ulbricht, M.; Yang, H. Porous polypropylene membranes with different carboxyl polymer brush layers for reversible protein binding via surface-initiated graft copolymerization. *Chem. Mater.* **2005**, *17*, 2622−2631.
(29) Na, C.; Park, H. Preparation of acrylic acid grafted polypropylene nonwoven fabric by photoinduced graft polymerization with preabsorption of monomer solution. *J. Appl. Polym. Sci.* **2009**, *114*, 387−397.
(30) Costamagna, V.; Wunderlin, D.; Larranaga, M.; Mondragon, I.; Strumia, M. Surface functionalization of polyolefin films via the ultraviolet-induced photografting of acrylic acid: Topographical characterization and ability for binding antifungal agents. *J. Appl. Polym. Sci.* **2006**, *102*, 2254−2263.
(31) Ma, H.; Davis, R.; Bowman, C. A novel sequential photoinduced living graft polymerization. *Macromolecules* **2000**, *33*, 331−335.
(32) Janorkar, A.; Metters, A.; Hirt, D. Modification of poly(lactic acid) films: Enhanced wettability from surface-confined photografting and increased degradation rate due to an artifact of the photografting process. *Macromolecules* **2004**, *37*, 9151−9159.
(33) Kang, E.; Tan, K.; Kato, K.; Uyama, Y.; Ikada, Y. Surface modification and functionalization of polytetrafluoroethylene films. *Macromolecules* **1996**, *29*, 6872−6879.
(34) Uchida, E.; Uyama, Y.; Ikada, Y. Sorption of low-molecular-weight anions into thin polycation layers grafted onto a film. *Langmuir* **1993**, *9*, 1121−1124.
(35) Bou, R.; Guardiola, F.; Codony, R.; Faustman, C.; Elias, R.; Decker, E. Effect of heating oxymyoglobin and metmyoglobin on the oxidation of muscle microsomes. *J. Agric. Food Chem.* **2008**, *56*, 9612−9620.
(36) Shantha, N. C.; Decker, E. A. Rapid, sensitive, iron-based spectrophotometric methods for determination of peroxide values of food lipids. *J. AOAC Int.* **1994**, *77*, 421−424.
(37) Alamed, J.; McClements, D. J.; Decker, E. A. Influence of heat processing and calcium ions on the ability of EDTA to inhibit lipid oxidation in oil-in-water emulsions containing omega-3 fatty acids. *Food Chem.* **2006**, *95*, 585−590.
(38) Panya, A.; Laguerre, M.; Lecomte, J.; Villeneuve, P.; Weiss, J. Effects of chitosan and rosmarinate esters on the physical and oxidative stability of liposomes. *J. Agric. Food Chem.* **2010**, *58*, 5679−5684.
(39) Gao, L.; McCarthy, T. Wetting 101 degrees. *Langmuir* **2009**, *25*, 14105−14115.
(40) Rangwalla, H.; Schwab, A.; Yurdumakan, B.; Yablon, D.; Yeganeh, M. Molecular structure of an alkyl-side-chain polymer-water interface: Origins of contact angle hysteresis. *Langmuir* **2004**, *20*, 8625−8633.
(41) Fasce, L. A.; Costamagna, V.; Pettarin, V.; Strumia, M.; Frontini, P. M. Poly(acrylic acid) surface grafted polypropylene films: Near surface and bulk mechanical response. *eXPRESS Polym. Lett.* **2008**, *2*, 779−790.
(42) Malaisamy, R.; Berry, D.; Holder, D.; Raskin, L.; Lepak, L. Development of reactive thin film polymer brush membranes to prevent biofouling. *J. Membr. Sci.* **2010**, *350*, 361−370.
(43) Tian, F.; Decker, E.; Goddard, J. Development of an iron chelating polyethylene film for active packaging applications. *J. Agric. Food Chem.* **2012**, DOI: 10.1021/jf204585f.
(44) Kontoghiorghes, G.; Pattichis, K.; Neocleous, K.; Kolnagou, A. The design and development of deferiprone (L1) and other iron chelators for clinical use: Targeting methods and application prospects. *Curr. Med. Chem.* **2004**, *11*, 2161−2183.
(45) Dubolazov, A.; Guven, O.; Pekel, N.; Azhgozhinova, G.; Mun, G. Electrochemical, spectroscopic, and thermal studies on interactions of linear poly(acrylic acid) with uranyl ions in aqueous solutions. *J. Polym. Sci. Part B: Polym. Phys.* **2004**, *42*, 1610−1618.
(46) Blcak, N.; Koza, G.; Atay, T. Metal chelating resins by condensation of ethylene diamine with p-dichloromethyl benzene. *J. Appl. Polym. Sci.* **1996**, *61*, 799−804.
(47) Kearsley, M. W.; Birch, G. G. Carbohydrate/iron complex formation. *Food Chem.* **1977**, *2*, 209−217.
(48) Masuda, S.; Miyahara, T.; Minagawa, K.; Tanaka, M. Polymerization and complexation of methacryloylglycine. *J. Polym. Sci., Part A: Polym. Chem.* **1999**, *37*, 1303−1309.
(49) Anonymous. *Code of Federal Regulations*; U.S. Government Printing Office: Washington, DC, 2002; Title 21, Part 172.